Surface Structures

DOI: 10.1002/anie.200903085

Resolving the Atomic Structure of Vanadia Monolayer Catalysts: Monomers, Trimers, and Oligomers on Ceria**

Martin Baron, Heather Abbott, Oleksandr Bondarchuk, Dario Stacchiola, Alexander Uhl, Shamil Shaikhutdinov, Hans-Joachim Freund, Cristina Popa, Maria Veronica Ganduglia-Pirovano,* and Joachim Sauer*

Supported vanadium oxide catalysts have received considerable attention owing to their high activity for selective oxidation reactions.[1–5] The reactivity has been shown to depend strongly on the oxide support,[2–5] with reducible oxides (e.g., ceria, titania, and zirconia) exhibiting much higher turnover frequencies for oxidative dehydrogenation (ODH) reactions than irreducible oxides (e.g., silica and alumina).[3,5] Structural characterization of the catalysts has been performed primarily using Raman and UV/Vis spectroscopy (see Ref. [4,6,7] and references therein), as well as X-ray absorption spectroscopy.[8] These results have been used to postulate that vanadia catalysts consist of isolated and polymer structures that wet the supporting oxide (so-called "monolayer catalysts"). To elucidate the surface chemistry of vanadia, different model systems, such as vanadia single crystals[9] and thin films[10] as well as vanadia clusters supported on planar metal oxide substrates,[11–15] have been studied experimentally by surface-science techniques and computational means.[16,17]

To rationalize structure–reactivity relationships, well-defined systems are required. Of the reducible metal oxide supports that are known to be highly active in ODH reactions, ceria is particularly suited, because well-ordered thin films can be grown with a known surface termination.[18,19] Previously, the structure and reactivity of vanadia supported on $CeO_2(111)$ has been studied using photoelectron spectroscopy (PES) and temperature-programmed desorption (TPD).[14,15] However, the atomic structure of ceria-supported vanadia monolayer catalysts has not been resolved.

Herein, using a combination of high-resolution scanning tunneling microscopy (STM), infrared reflection absorption spectroscopy (IRAS), and PES with synchrotron radiation, we unambiguously demonstrate the formation of monomeric $O{=}V^{5+}O_3$ species on the $CeO_2(111)$ surface at low vanadia loadings. For the first time, we show a direct relationship between the nuclearity of vanadia species (monomeric vs. polymeric) as observed by STM and their vibrational properties. We show that ceria stabilizes the vanadium +5 oxidation state, leading to partially reduced ceria upon vanadium deposition. These experimental results are fully supported by density functional theory (DFT) calculations. The results indicate that ceria surfaces stabilize small vanadia species, such as monomers and trimers, that sinter into two-dimensional, monolayer islands. Such stabilization probably plays a crucial role in the enhanced activity observed for ceria-supported vanadia in ODH reactions. Indeed, low-nuclearity species revealed reactivities at much lower temperatures[20] than those with higher nuclearity, which in turn show strong similarities to the reactivity of vanadia clusters supported on alumina and silica.[11,13]

Figure 1 presents compelling evidence for the presence of vanadia monomers on ceria at low coverage (ca. 0.3 V atoms nm^{-2}). The STM image in Figure 1a shows that highly dispersed and randomly distributed species are formed upon deposition of vanadium in an ambient oxygen atmosphere onto a $CeO_2(111)$ thin film (see the Experimental Section). The absence of preferential nucleation sites indicates a strong interaction between vanadia species and the underlying ceria support. In the atomically resolved image (inset of Figure 1a), the two protruding spots (ca. 3 Å in diameter and 1.2 Å in height) appear to be monomers positioned atop protrusions in the ceria substrate. The apparent height of these vanadia species depends on the tunneling bias and monotonically decreases from approximately 1.8 Å at 2.2 V to approximately 0.9 Å at 3 V. At certain voltages, a dark "halo" is visible around a few of the monomeric species (see Figure 1a), which may be related to defect structures of the ceria film.[19]

The IR spectrum corresponding to the sample shown in Figure 1a is depicted in Figure 1d with an absorption feature at 1006 cm^{-1}. This peak is assigned to the vanadyl (V=O) stretching vibration on the basis of comparison with other vanadia systems and reference compounds in which the V=O

[*] M. Baron, Dr. H. Abbott, Dr. O. Bondarchuk, Dr. D. Stacchiola,[+] Dr. A. Uhl, Dr. S. Shaikhutdinov, Prof. Dr. H.-J. Freund
Fritz Haber Institute of the Max Planck Society
Chemical Physics Department
Faradayweg 4–6, 14195 Berlin (Germany)
Fax: (+49) 30-8413-4105
E-mail: shamil@fhi-berlin.mpg.de
Dr. C. Popa, Dr. M. V. Ganduglia-Pirovano, Prof. Dr. J. Sauer
Humboldt-Universität zu Berlin, Department of Chemistry
Unter den Linden 6, 10009 Berlin (Germany)
E-mail: h34600ox@chemie.hu-berlin.de
[+] Present address:
Michigan Technological University, Department of Chemistry
1400 Townsend Dr., Houghton, MI 49931 (USA)

[**] This work has been supported by the Deutsche Forschungsgemeinschaft (SFB 546, "Transition Metal Oxide Aggregates"). We recognize Dr. Helmut Kuhlenbeck for technical assistance at BESSY II. H.A. and D.S. gratefully acknowledge fellowship support by the Alexander von Humboldt Foundation.

Supporting information for this article is available on the WWW under http://dx.doi.org/10.1002/anie.200903085.

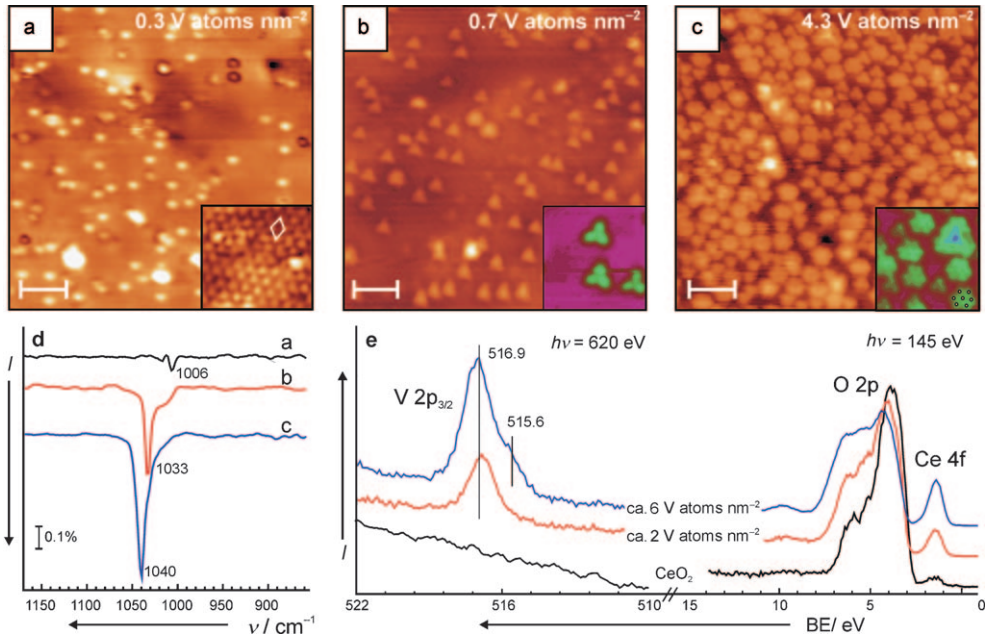

Figure 1. a–c) STM images of $VO_x/CeO_2(111)$ for various vanadia loadings as indicated. Sample (a) was annealed to 300 K, while samples (b) and (c) were annealed to 700 K. The insets highlight the atomic structure of the vanadia deposits. The scale bars are 3 nm. Tunneling bias is 3 V; tunneling current is 0.02 nA (a), 0.01 nA (b), and 0.10 nA (c). d) IRA spectra of the vanadyl (V=O) stretching region for the corresponding STM images. e) PE spectra for two loadings of vanadia on $CeO_2(111)$ compared to a pristine $CeO_2(111)$ thin film.

stretch falls into the region between 990 and 1040 cm^{-1}.[2,5] The IR spectroscopy results suggest that the vanadia monomers observed by STM are positioned with the vanadyl group perpendicular to the substrate.

Furthermore, photoelectron spectroscopy of the VO_x/CeO_2 samples at lower vanadia coverage for these measurements reveals vanadium only in a fully oxidized, +5 state, as shown by a single peak at approximately 517 eV for the V $2p_{3/2}$ core level[21] (Figure 1e). In agreement with previous observations,[15,22] the V deposition is accompanied by reduction of Ce in the CeO_2 film, as indicated by an increase in the intensity of the Ce 4f peak in the PE spectrum shown in Figure 1e. The intensity of this peak is directly correlated to the Ce^{3+} concentration.[23]

Although the V 3d band and the Ce 4f band have very similar binding energies,[21] a contribution from vanadium in this region can be excluded, as vanadium is in a +5 oxidation state and, therefore, the V 3d band is empty. In this scenario, Ce–O bonds are weakened through the formation of V–O bonds, resulting in partial Ce reduction.

Thus, these results are consistent with a previously suggested model for monomeric vanadia species, in which tetrahedral VO_4 is anchored to the surface through three O atoms bound to Ce atoms in the film, with one V=O group pointing off the surface.[5]

Increasing vanadia coverage at low temperatures first resulted in a higher density of monomeric species and the simultaneous formation of dimers, trimers, and ill-defined large aggregates with a relatively broad size distribution (not shown here). The latter species indicate kinetically limited growth of the vanadia particles. Upon heating to elevated temperatures, the monomeric species sintered. Therefore, higher coverages of vanadia on ceria were investigated after annealing to 700 K to create stable particles that could be used in reactivity studies.[24]

The STM picture in Figure 1b shows roughly twice the amount of vanadia as deposited in Figure 1a (i.e., 0.7 V atoms nm^{-2}). Annealing to 700 K caused monomers to sinter, ultimately producing vanadia trimers, as illustrated more clearly by the inset of Figure 1b. The distance between the spots within the trimers is (3.9 ± 0.2) Å, that is, within the range of the lattice constant for $CeO_2(111)$ (3.9 Å) and the distance for the nearest V=O species in $V_2O_5(001)$ (3.5–3.6 Å). The apparent height of the trimers was found to be (1.0 ± 0.3) Å at 3.0 V, that is, about the same as for monomers, thus indicating that the trimers are anchored flat on the surface.

The IR spectrum corresponding to the sample in Figure 1b has a vanadyl stretch absorption peak at 1033 cm^{-1}, that is, blue-shifted by approximately 25 cm^{-1} as compared to the monomeric species. This shift can, in principle, be attributed to the onset of dipole coupling between neighboring V=O groups in the trimers.

A few even larger vanadia species, consisting of seven protrusions, are also visible in the middle of Figure 1b. The number of these heptamers increases as the coverage is increased further (to 4.3 V atoms nm^{-2}, Figure 1c). The heptamers have a hexagonal shape, a lateral distance of (3.7 ± 0.2) Å between the protrusions, and an apparent height of (1.3 ± 0.3) Å at 3.0 V, that is, about the same as for trimers, as shown in the inset of Figure 1c. (Note that the coexistence of trimers, heptamers, and oligomers, clearly seen in the inset of Figure 1c, indicates that these species are surface structures and not merely electronic effects.) The edges of the vanadia deposits are aligned along the main crystallographic directions of the $CeO_2(111)$ surface underneath. Moreover, the orientation of trimers follows the rotational domain structure of the ceria films. These findings suggest that V=O groups in monomers, trimers, and oligomers occupy the same sites with respect to the ceria substrate.

The central part of the largest cluster shown in the inset of Figure 1c has an apparent height of (2.3 ± 0.3) Å, approximately twice the height of monomers and trimers. The growth of multilayer vanadia particles on ceria at high coverages could explain the presence of the low binding

energy shoulder in the V 2p region, which corresponds to vanadium in a +3 oxidation state (Figure 1e). Concomitantly, the PES band at approximately 2 eV gains intensity owing to either further reduction of Ce, occupation of the V 3d valence band, or both.

At high coverage (4.3 V nm^{-2}), the frequency of the V=O stretch shifts further to 1040 cm^{-1}, ultimately approaching the frequencies (ca. 1045 cm^{-1}) observed for vanadia deposits on nonreducible silica and alumina thin films,[11,12] where three-dimensional, V=O terminated V_2O_3 nanoparticles dominate the structure, and for V=O terminated V_2O_3(0001) surfaces.[25]

Thus, the combined STM and IRAS results clearly show the blue shift of the vanadyl frequency upon increasing vanadia cluster size from mono- to polyvanadates. This result contrasts with previous assignments for vanadia/ceria powder catalysts, where the lower Raman frequency (1017 cm^{-1}) was assigned to polymeric species and the higher (1034 cm^{-1}) to isolated species.[3,7] However, the latter assignment was based exclusively on spectroscopic studies as a function of vanadia loading, whereas in the present study monomeric species were directly imaged by STM, and a direct structure–spectroscopy correlation could be established.

Our DFT results are consistent with the experimental observations for vanadia monomers and trimers. When a V atom is deposited on the nondefective CeO_2(111) surface, as many as four electrons are transferred from V 3d states into Ce 4f states, thus creating four Ce^{3+} ions and leaving vanadium in the +4 oxidation state, as indicated by the presence of one electron in the d states (Figure 2a). There is, however, an isomeric structure of the V/CeO_2(111) system with much lower energy (1.48 eV less) in which oxygen atoms have rearranged. A vanadyl bond is formed and a subsurface oxygen defect is created in the third oxygen layer (Figure 2a). This structure possesses five Ce^{3+} ions and V in the +5 oxidation state. These V=O species on the defective CeO_2-(111) surface (i.e., the ceria surface with an inner-layer oxygen vacancy) are predicted to be the thermodynamically stable monomers under strongly reducing conditions (ultra-high vacuum (UHV) and high temperature).[26] For milder conditions (in the presence of O_2 and at lower temperature), V=O species on the nondefective CeO_2(111) surface become stable. In this system, vanadium is also stabilized in the +5 oxidation state by transferring three electrons into Ce 4f states, thus creating three Ce^{3+} ions (Figure 2b). The important finding is that regardless of whether V or any VO_n species are deposited onto the CeO_2(111) surface, ceria always stabilizes the vanadium +5 oxidation state (see Ref. [26] for $n>1$).

The V=O species of both the V/CeO_2 and VO/CeO_2 systems are positioned in a threefold hollow site above the surface oxygen atoms and atop the subsurface oxygen atoms of the ceria substrate pointing off the surface. They are anchored to the surface through three O atoms (V-O-Ce^{3+} bonds). The VO/CeO_2 structure shown in Figure 2b has already been predicted in reference [17] with a very similar V=O vibrational frequency (1051 cm^{-1} vs. 1052 cm^{-1} presented herein). In agreement with experiment, this monomer frequency is significantly smaller than the VO frequencies calculated for the vanadyl-terminated V_2O_3 surface (1072 cm^{-1}) or the V_2O_5(001) surface (1079–1095 cm^{-1}).[27]

For the vanadia trimers shown in Figure 2c, the V=O groups are similarly positioned as in monomers and are also anchored by V-O-Ce^{3+} bonds. Similar to the monomers, the vanadium centers are also stabilized in the +5 oxidation state. In the trimers, the vanadyl stretch frequency is blue-shifted by approximately 35 cm^{-1} compared to that for the two monomeric species of Figure 2a,b (see the Supporting Information), thus confirming the above assignment of the experimental IRA spectra.

In summary, the formation of vanadyl-terminated monomers, trimers, and oligomers on the CeO_2(111) surface at submonolayer surface coverage is shown, and the atomic structure of vanadia/ceria surfaces has been resolved to a far greater extent using a combination of high-level experimental and theoretical results. A direct relationship between the morphology of vanadia/ceria and the vanadyl frequency, observed here for a model system, allows us to link the structure of vanadia surface species and the characterization of real catalysts by Raman and IR spectroscopy in a more definitive manner. The results clearly show that ceria surfaces stabilize small vanadia species in a +5 oxidation state, which wet and reduce the ceria surface and probably play a crucial role in the enhanced reactivity observed for ceria-supported vanadia in ODH reactions.

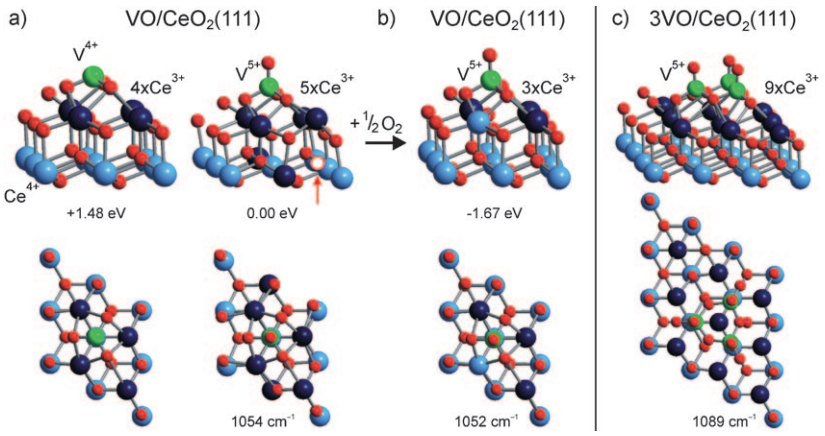

Figure 2. Side and top views of a) V, b) VO, and c) 3VO species on CeO_2(111). V/CeO_2 calculations approximate UHV deposition, while VO/CeO_2 calculations approximate deposition in an ambient O_2 atmosphere. Ce^{4+} light blue, Ce^{3+} dark blue, V green (oxidation state indicated), O red. An arrow and open circle indicate the oxygen vacancy. The (unscaled) vanadyl stretching frequencies for the corresponding structures is indicated. The (2×2) and the (3×3) surface unit cells used in the calculations are shown.

Experimental Section

The experiments were carried out in a UHV chamber (base pressure ca. 2×10^{-10} mbar) equipped with low-energy electron diffraction (LEED), X-ray PES, IRAS, and STM. The well-ordered CeO_2(111) thin films were grown on a Ru(0001)

substrate as described previously.[19,28] Vanadium (Goodfellow, 99.8%) was deposited by physical vapor deposition in 10^{-6} mbar O_2 onto a fully oxidized ceria film approximately 3 nm thick at approximately 110 K. The samples were then annealed to 300 K in the same oxygen atmosphere. The STM measurements were performed at room temperature, while the IRAS measurements were conducted at approximately 110 K. The PES experiments using synchrotron radiation were performed on identically prepared samples in another UHV chamber at BESSY II (beamline UE52-PGM1) with a Scienta R4000 analyzer (energy resolution below 200 meV). The energy was calibrated by setting the Au $4f_{7/2}$ level to 84.0 eV for a Au foil.

The spin-polarized calculations were performed using the DFT (PBE) + U approach as implemented in the VASP package.[29] A value of 4.5 eV was used for the Hubbard U parameter. The projector augmented wave method (PAW) was used at a plane-wave cutoff of 400 eV to decouple the core from valence electrons. The Ce (4f, 5s, 5p, 5d, 6s), O (2s, 2p), and V (3p, 3d, 4s) electrons were treated as valence states. For the Brillouin zone integration, a $(3\times3\times1)/(2\times2\times1)$ *k* mesh was used for the $(2\times2)/(3\times3)$ structures.

The $CeO_2(111)$ surface was modeled by a supercell with nine atomic layers with calculated CeO_2 bulk equilibrium lattice constants[30] and a vacuum thickness of approximately 13 Å. For the $m\,VO_n/CeO_2(111)$ structures (2×2) and (3×3) surface unit cells were employed. VO_n(g) species were adsorbed on the clean and defective $CeO_2(111)$ surfaces,[26] and the lowest-energy structure for a given stoichiometry was found. The atoms in the six top layers were allowed to relax, and those in the three bottom layers were fixed to their positions in the bulk.

The vibrational modes were obtained by finite differences of the forces with atomic displacements of 0.02 Å.

Received: June 8, 2009
Revised: August 12, 2009
Published online: September 18, 2009

Keywords: density functional calculations · nanoparticles · structure elucidation · surface chemistry · thin films

[1] G. Deo, I. E. Wachs, J. Haber, *Crit. Rev. Surf. Chem.* **1994**, *4*, 141; A. Khodakov, B. Olthof, A. T. Bell, E. Iglesia, *J. Catal.* **1999**, *181*, 205; M. V. Martinez-Huerta, G. Deo, J. L. G. Fierro, M. A. Bañares, *J. Phys. Chem. C* **2008**, *112*, 11441.
[2] B. Olthof, A. Khodakov, A. T. Bell, E. Iglesia, *J. Phys. Chem. B* **2000**, *104*, 1516.
[3] M. A. Bañares, M. V. Martinez-Huerta, X. T. Gao, I. E. Wachs, J. L. G. Fierro in *Studies in Surface Science and Catalysis*, *Vol. 130D* (Eds.: A. Corma, F. V. Melo, S. Mendioroz, J. L. G. Fierro), Elsevier, Amsterdam, **2000**, pp. 3125.
[4] B. M. Weckhuysen, D. E. Keller, *Catal. Today* **2003**, *78*, 25.
[5] I. E. Wachs, *Catal. Today* **2005**, *100*, 79.
[6] G. T. Went, S. T. Oyama, A. T. Bell, *J. Phys. Chem.* **1990**, *94*, 4240; S. C. Su, A. T. Bell, *J. Phys. Chem. B* **1998**, *102*, 7000; E. L. Lee, I. E. Wachs, *J. Phys. Chem. C* **2008**, *112*, 6487; H. S. Kim, S. A. Zygmunt, P. C. Stair, P. Zapol, L. A. Curtiss, *J. Phys. Chem. C* **2009**, *113*, 8836; B. Kilos, A. T. Bell, E. Iglesia, *J. Phys. Chem. C* **2009**, *113*, 2830; D. Keller, T. Visser, F. Souilimani, D. C. Köningsberger, B. M. Weckhuysen, *Vib. Spectrosc.* **2007**, *43*, 140.
[7] M. A. Bañares, G. Mestl, *Adv. Catal.* **2009**, *52*, 43.
[8] D. E. Keller, S. M. K. Airaksinen, A. O. Krause, B. M. Weckhuysen, D. C. Koningsberger, *J. Am. Chem. Soc.* **2007**, *129*, 3189; M. Ruitenbeek, A. J. van Dillen, F. M. F. de Groot, I. E. Wachs, J. W. Geus, D. C. Koningsberger, *Top. Catal.* **2000**, *10*, 241.
[9] K. Devriendt, H. Poelman, L. Fiermans, *Surf. Sci.* **1999**, *435*, 734; R. P. Blum, H. Niehus, C. Hucho, R. Fortrie, M. V. Ganduglia-Pirovano, J. Sauer, S. Shaikhutdinov, H. J. Freund, *Phys. Rev. Lett.* **2007**, *99*, 226103.
[10] S. Surnev, M. G. Ramsey, F. P. Netzer, *Prog. Surf. Sci.* **2003**, *73*, 117; H. Niehus, R. P. Blum, D. Ahlbehrendt, *Surf. Rev. Lett.* **2003**, *10*, 353; A. C. Dupuis, M. Abu Haija, B. Richter, H. Kuhlenbeck, H. J. Freund, *Surf. Sci.* **2003**, *539*, 99.
[11] N. Magg, B. Immaraporn, J. B. Giorgi, T. Schroeder, M. Baumer, J. Dobler, Z. L. Wu, E. Kondratenko, M. Cherian, M. Baerns, P. C. Stair, J. Sauer, H. J. Freund, *J. Catal.* **2004**, *226*, 88.
[12] S. Kaya, Y. N. Sun, J. Weissenrieder, D. Stacchiola, S. Shaikhutdinov, H. J. Freund, *J. Phys. Chem. C* **2007**, *111*, 5337.
[13] Y. Romanyshyn, S. Guimond, H. Kuhlenbeck, S. Kaya, R. P. Blum, H. Niehus, S. Shaikhutdinov, V. Simic-Milosevic, N. Nilius, H. J. Freund, M. V. Ganduglia-Pirovano, R. Fortrie, J. Dobler, J. Sauer, *Top. Catal.* **2008**, *50*, 106.
[14] G. S. Wong, M. R. Concepcion, J. M. Vohs, *J. Phys. Chem. B* **2002**, *106*, 6451; T. Feng, J. M. Vohs, *J. Catal.* **2004**, *221*, 619.
[15] J. M. Vohs, T. Feng, G. S. Wong, *Catal. Today* **2003**, *85*, 303.
[16] M. Calatayud, B. Mguig, C. Minot, *Surf. Sci.* **2003**, *526*, 297; A. Vittadini, M. Casarin, M. Sambi, A. Selloni, *J. Phys. Chem. B* **2005**, *109*, 21766; T. K. Todorova, M. V. Ganduglia-Pirovano, J. Sauer, *J. Phys. Chem. C* **2007**, *111*, 5141; M. M. Islam, D. Costa, M. Calatayud, F. Tielens, *J. Phys. Chem. C* **2009**, *113*, 10740; J. Döbler, M. Pritzsche, J. Sauer, *J. Phys. Chem. C* **2009**, *113*, 12454.
[17] V. Shapovalov, H. Metiu, *J. Phys. Chem. C* **2007**, *111*, 14179.
[18] D. R. Mullins, P. V. Radulovic, S. H. Overbury, *Surf. Sci.* **1999**, *429*, 186.
[19] J. L. Lu, H. J. Gao, S. Shaikhutdinov, H. J. Freund, *Surf. Sci.* **2006**, *600*, 5004.
[20] M. V. Ganduglia-Pirovano, C. Popa, J. Sauer, H. L. Abbott, A. Uhl, M. Baron, D. Stacchiola, O. Bondarchuk, S. Shaikhutdinov, H. J. Freund, unpublished results.
[21] S. Guimond, J. M. Sturm, D. Gobke, Y. Romanyshyn, M. Naschitzki, H. Kuhlenbeck, H. J. Freund, *J. Phys. Chem. C* **2008**, *112*, 11835.
[22] M. V. Martinez-Huerta, J. M. Coronado, M. Fernandez-Garcia, A. Iglesias-Juez, G. Deo, J. L. G. Fierro, M. A. Bañares, *J. Catal.* **2004**, *225*, 240.
[23] A. Pfau, K. D. Schierbaum, *Surf. Sci.* **1994**, *321*, 71; D. R. Mullins, S. H. Overbury, D. R. Huntley, *Surf. Sci.* **1998**, *409*, 307.
[24] M. V. Ganduglia-Pirovano, J. L. F. Da Silva, J. Sauer, *Phys. Rev. Lett.* **2009**, *102*, 026101.
[25] S. Guimond, M. Abu Haija, S. Kaya, J. Lu, J. Weissenrieder, S. Shaikhutdinov, H. Kuhlenbeck, H. J. Freund, J. Dobler, J. Sauer, *Top. Catal.* **2006**, *38*, 117.
[26] C. Popa, M. V. Ganduglia-Pirovano, J. Sauer, unpublished results.
[27] M. Abu Haija, S. Guimond, Y. Romanyshyn, A. Uhl, H. Kuhlenbeck, T. K. Todorova, M. V. Ganduglia-Pirovano, J. Dobler, J. Sauer, H. J. Freund, *Surf. Sci.* **2006**, *600*, 1497; V. Brázdová, M. V. Ganduglia-Pirovano, J. Sauer, *Phys. Rev. B* **2004**, *69*, 165420. Note that harmonic V=O frequencies calculated by DFT are systematically higher than observed frequencies, which has been taken into account by using scale factors such as 0.967 or 0.958. Here we refer to unscaled frequencies.
[28] M. Baron, O. Bondarchuk, D. Stacchiola, S. Shaikhutdinov, H.-J. Freund, *J. Phys. Chem. C* **2009**, *113*, 6042.
[29] vasp.5.1.49 ed., http://cms.mpi.univie.ac.at/vasp/.
[30] J. L. F. Da Silva, M. V. Ganduglia-Pirovano, J. Sauer, V. Bayer, G. Kresse, *Phys. Rev. B* **2007**, *75*, 045121.

